Scientific Research Publishing

International Journal of Geosciences, 2025, 16(9), 636-657
https://www.scirp.org/journal/ijg
ISSN Online: 2156-8367
ISSN Print: 2156-8359

Diagnosis of a Small Dam Using Electric and Electromagnetic Methods

—Case of Gonsé Dam (Central Region, Burkina Faso)

Maxime Wubda, Youssouf Koussoubé, Julien Nikiema, Soumaila Paré

Laboratoire Géosciences et Environnement (LaGE), Université Joseph Ki-Zerbo, Ouagadougou, Burkina Faso
Email: mwubda@gmail.com

How to cite this paper: Wubda, M., Koussoubé, Y., Nikiema, J. and Paré, S. (2025) Diagnosis of a Small Dam Using Electric and Electromagnetic Methods—Case of Gonsé Dam (Central Region, Burkina Faso). *International Journal of Geosciences*, **16**, 636-657.
https://doi.org/10.4236/ijg.2025.169031

Received: July 11, 2025
Accepted: September 25, 2025
Published: September 28, 2025

Abstract

Burkina Faso is a Sahelian country in West Africa that is faced with water resource mobilization problems. To develop vital sectors of its economy such as agriculture and livestock breeding, the country has elected to mobilize surface water through the construction of small earthen dams. With a stock of almost a thousand dams, the country is now faced with the problem of ageing structures, with embankments sometimes breaking during periods of high flooding. To deal with this situation, Burkina Faso has taken action to rehabilitate its dams. The planned maintenance work will, however, require prior diagnostics, which, given the number of structures to be examined, will constitute a real challenge. On this subject, geophysics offers detection methods that can be applied to the diagnosis of internal erosion problems that frequently affect earthen dams. In this regard, the study of the small Gonsé dam illustrates the contribution of geophysical methods to the detection of areas of water leaks through an earthen embankment. It demonstrates that, with the use of electromagnetic and electrical methods, it is possible to establish an initial diagnosis of structures through a routine of simple, rapid and non-invasive measurements.

Keywords

Burkina Faso, Gonsé Dam, Geophysics, Electromagnetism, Electrical Resistivity

1. Introduction

Water supply in the Sahelian countries is an important component of the development policies implemented by these countries. Burkina Faso, located in this geographical zone, also faces difficulties in mobilizing and managing its water re-

sources [1].

In order to promote two of its vital sectors, namely agriculture and livestock farming, and to ensure the supply of drinking water to its cities, Burkina Faso has opted to mobilize surface water through the construction of water retention structures [2]. Thus, the first dam was built in the 1900s, and till 2011, according to an inventory by the Ministry of the Environment, Water and Sanitation [3], the country had nearly 1001 dams. Between 2011 and 2020, a further 34 structures were built, bringing the total number to 1035 dams.

Among all these infrastructures, three are hydroelectric dams, distinguished by their large capacity: Kompienga dam (2 billion cubic meters), Bagré dam (1.7 billion cubic meters) and Samandéni dam (1.5 billion cubic meters).

On the other hand, the structures that were built in large numbers are small dams made with homogeneous earthen (laterite) embankments, and their capacities are less than 1 million cubic meters. According to the national dam maintenance and safety strategy manual, published in 2022 by the Ministry of Environment, Water and Sanitary [4], they constitute nearly 87% of the national park. Inexpensive and easy to build, their model is based on the obstruction of a watercourse using a homogeneous earthen embankment, equipped with a central or lateral spillway [5]. There are no standards in the country governing the construction of these small dams, but rather proven construction techniques [5] that serve as good practice in the design and construction of these structures such as, the use of laterite (a material that is easy to compact and abundant in nature) for the construction of embankments and the adoption of open concrete spillways for flood drainage. Furthermore, it is difficult to say that good construction techniques are always used in the building of structures, as there are many actors involved in the field (state institutions, NGOs, individuals) and practically no monitoring, especially when construction projects are carried out by non-state actors.

As a result of non-compliance with construction techniques, misuse or natural aging, the current situation shows a stock of structures in poor condition with nearly 48% of them in an advanced state of degradation, which causes ruptures of dams every rainy season. This observation encourages the government to finally adopt a maintenance procedure manual for structures in 2024, and also to rehabilitate the office in charge of the construction and maintenance of hydraulic infrastructure (ONBAH) in May 2024, for the construction of future dams and the maintenance of those already existing.

For the rehabilitation of a number of fairly high dams that constitute the national park, it is necessary to have a fast and precise diagnostic method that can be used on a small scale. For small dams made with homogeneous soil, there are numerous physical pathologies (erosion of dikes, subsidence or cracking of the spillway, siltation of the basin, etc.), but most of them are detectable by simple visual observations. Those invisible concerns water leaks through dikes and/or spillways resulting from internal erosion or initial construction defects. For these latter cases, the recourse to in-depth investigations is necessary.

In the field of dam monitoring, several techniques exist. It includes the use of temperature [6], tracers [7], or certain geophysical methods such as electrical or electromagnetic resistivity [8] [9]. All the methods cited below, are not non-invasive or easy to use. However, at the time of rehabilitation, it is often a question of targeting damaged areas to be repaired urgently and as a priority, while avoiding disturbing the unaffected parts as much as possible.

The objective of this study is therefore to demonstrate, through a specific implementation, that geophysical exploration based on electrical or electromagnetic methods, already commonly used in dam siting studies [10] [11], can also constitute tools for fast, effective and above all, non-invasive diagnosis for dams to be controlled. It aims to show the effectiveness of a detection technique that allows, through a minimum of measurements, a rapid targeting of damaged areas which can be the subject of more in-depth investigation or future rehabilitation. In this respect, it uses the example of the diagnosis of the small Gonsé dam, which is a structure about fifteen years old, showing apparent signs of aging and which would undoubtedly need repair work in a fairly short period of time, that will help extend its lifespan.

2. Materials and Methods

2.1. Materials

2.1.1. The Study Site

- Site selection

The site selected for this study is the small dam of the Gonsé village. This dam is a representative structure of small water reservoirs with homogeneous compacted laterite embankment, built in large numbers in the country. It was built in 2006 and, like many structures of the same age, shows obvious signs of age. Due to its location in the peri-urban area of Ouagadougou, it suffers (compared to structures in rural areas) from significant anthropogenic impact due to the heavy demand from the large population nearby. It also illustrates the case of all these small dams which are used a lot and paradoxically, poorly monitored and maintained.

- General context

The context of our study site is the Gonsé hydrographic watershed (Cf; **Figure 1**). It is so named in reference to the name of the village where its outlet is located. It is a sub-basin of the Massili watershed, itself included in Nakanbé watershed. Located about thirty kilometers east of the city of Ouagadougou, this watershed of around 62 km^2 of surface, is between the coordinates (WGS 84-UTM 30 P-m) 1377500 N to 1387200 N, and 680180 E to 689100 E. Its outlet, in the south of the village of Gonsé, is located according to the coordinates 1378850 N and 683025 E. The site is accessible by the National Road 4 (RN4, Fada road) and the Departmental road 40 (D40, Boudtenga to Ziniaré).

The watershed straddles three municipalities: Saaba, Loumbila and Ziniaré. In addition to Gonsé, there are also the villages of Boudtenga, Loango, Samandin,

etc. These villages are occupied by populations mainly practicing agriculture and livestock and not fishing despite the presence of the dam on the site. The common language used in the area is Moore.

The climate of the study area is classified as Sudano-Sahelian, characterised by an annual alternation of two seasons: a long dry season from October to May and a shorter rainy season from June to September. The annual rainfall average over a ten-year period (2009 - 2018) of the meteorological station closest to the site (Ouagadougou) is 870 mm [12].

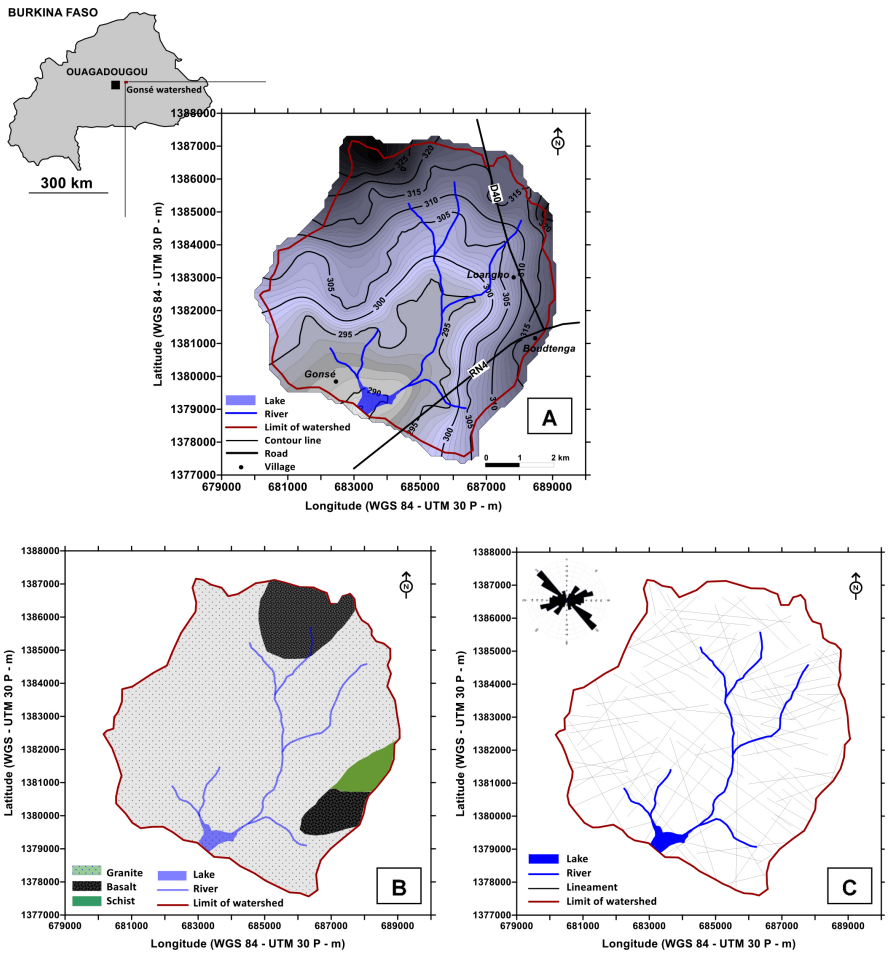

Figure 1. Gonsé watershed maps: Location and characteristics. (A) Topography (extracted from topographic map of Ouagadougou in 1/200,000, 2012; (B) Lithological context (extracted from geological map of Ouagadougou at 1/200,000, 2003; (C) Lineaments (extracted from ALOS Palsar images, 2016).

Morphologically, the Gonsé watershed is a unit with few contrasts. Alevations range between 280 and 350 meters (Cf; **Figure 1(A)**) with the highest points comprising the summits of armored hillocks, which reach heights between 20 and 30 meters. These hillocks are prominent features in the villages of Boudtenga and Loango.

In the north-east of the site, particularly in the village of Loango and its sur-

rounding areas, we also observe small rocky outcrops (10 to 500 m^2), mainly granitic and scattered throughout the landscape. They appear in the form of blunt pellets (oriented N30˚), or large fractured blocks. The largest ones dominate the topography by barely 5 meters. These outcrops represent the visible parts of a highly fractured geological bedrock (Cf; **Figure 1(C)**), dominated by plutonic rocks of Birimian origin (biotite granites, granodiorites, pegmatites). Additionally, volcanic rocks (basalts) are present in the northern and eastern regions of the site, while metamorphic rocks (schists) are found in the far east (see **Figure 1(B)**).

Apart from these minor reliefs, the rest of the landscape shows very gently sloping glacis at the bottom of which, the hydrographic network made up of faint gullies (Cf; **Figure 1(A)**) is located.

- The geophysical measurements site

The geophysical exploration zone corresponds to the installation area of Gonsé dam (Cf; **Figure 2**). It is located in the south of the watershed (Cf; **Figure 2(A)**). The dam built there is a small water retention structure, consisting of a basin and a homogeneous compacted earth embankment (Cf; **Figure 2(F)**), 500 meters long, and oriented SSE-NNW.

The embankment obstructs a main river flowing from north to south. In its central part, it has a reinforced concrete spillway, 105 meters long (Cf; **Figure 2(E)**). The embankment also serves as a road connecting the heart of the village to the hamlets located in the southern part of the dam.

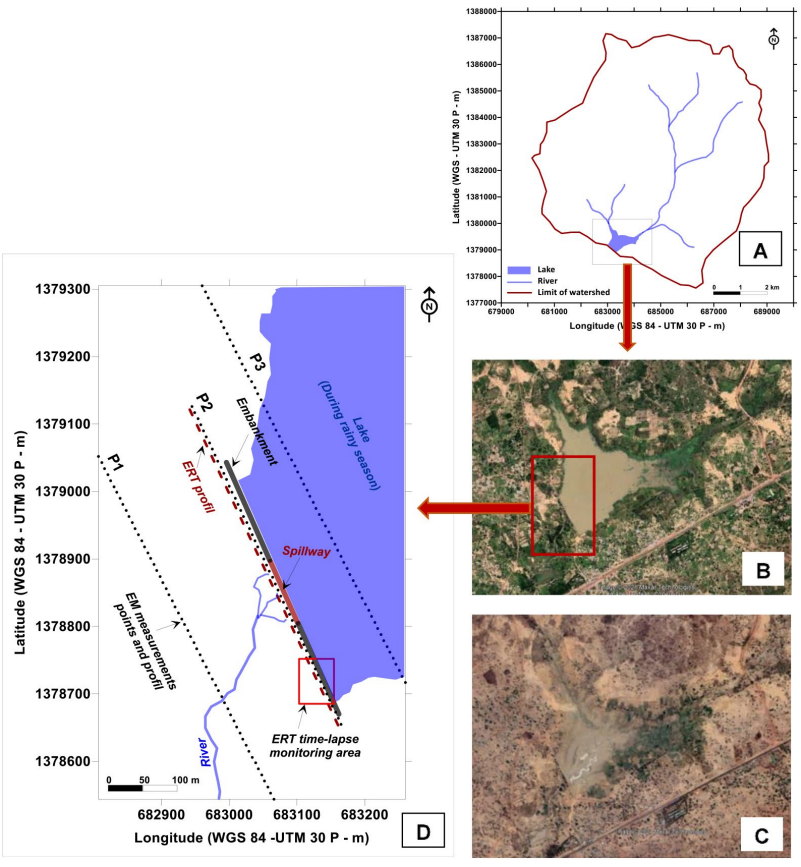

Figure 2. Site of Gonsé dam. (A) Location; (B) The dam site during the rainy season (Google Earth image, September 2023); (C) The site during the dry season (Google Earth image, March 2023); (D) Geophysical exploration area; (E) View of the lake and concrete spillway; F), view of the southern section of the earthen embankment.

The dam basin upstream of the embankment covers an area of approximately 0.6 km^2. It is largely filled with clay deposits whose thickness in some places reaches 60 centimeters. Due to its shallow depth (0.6 meters on average), the basin fills quite quickly at the beginning of the rainy season (June) and forms a small lake (Cf; **Figure 2(B)**) with a storage volume of approximately 376,000 m^3. However, all this water is only available for a few months during the dry season (until February). By the end of March, the basin is often already dry (Cf; **Figure 2(C)**).

The part of the site downstream of the embankment is a shallow valley, drained by the extension of the watercourse (obstructed by the embankment) which evacuates excess floods from the dam passing through the spillway. The route of the watercourse in contact with the embankment has been modified by the construction of a dissipation basin from which several drains start. This entire downstream section is quite wooded, with the presence of a gallery forest along the banks of the watercourse. Further from the banks, we observe a few plots of market gardening, irrigated through a water intake, located on the north side of the embankment.

In the dam installation site, no rock outcrops were observed to directly confirm the presence of a granitic bedrock as indicated on the lithological map in **Figure 1(D)**. Only the nature of the materials (quartz grains, slightly altered biotite) seen on some termites and ant nests encountered, tends to confirm this presence. Due to the lack of superficial clues, the level of fracturing and the directions of fractures were difficult to verify in the field. Only one supposed lineament was observed in the north of the embankment. It is marked by a northeast, southwest alignment of large trees and termite mounds and seems to correspond to one of the lineaments present on the lineament map in **Figure 1(B)**.

Geophysical studies that were carried out at the dam site, focused specifically on the neighboring parts of the embankment. This is a small area of 750 meters long (from north to south) and 400 meters wide (from east to west), in which the embankment of the dam is centred with a diagonal orientation (Cf; **Figure 2(D)**.

2.1.2. Mapping Tools

To create maps for this study, we used the following specific support:

- ALOS PALSAR satellite image (AP_07496_FBD_F0230_RT1, 2016) to identify the lineaments of the site;
- ENVI software (Geospatial software) for processing satellite images;
- SURFER software (Golden software) for the spatialization of geophysical exploration data and the production of all maps (lineaments and geophysical parameters).

Some input data, such as the values of geophysical parameters as well as the coordinates of measurement points taken on the site, were entered into an Excel spreadsheet, and then imported into the mapping software database.

2.1.3. Geophysical Equipment

It consists of exploration equipment and data processing tools.

- Exploration equipment

It includes an electromagnetic measuring device, the Max-Min II, and a direct current electrical measuring device, the Syscal Pro 48 to which we have attached a GPS for positioning the measurement points.

➢ *Max-Min II*

It is an electromagnetic prospecting device in the frequency domain from the manufacturer Apex. It consists of two parts:

- A transmitter part, which includes a transmitting device connected to a circular coil. It allows the generation of a primary electromagnetic field in 110, 220, 440, 880, 1760, 3520, 7040 and 14080 hertz;
- A receiver part, consisting of two antennas connected to a receiving device which integrates a conductivity reading module. It allows readings of field values in Inphase (%) and Outphase (%), and also conductivity values (mS/m) which can be converted later into resistivities (Ohm.m);
- These two parts are connected by a cable of length which can be 50, 75 or 100 meters.

This equipment can be used in survey mode or sounding mode.

➢ *Syscal Pro* 48

Syscal is a resistivimeter produced by IRIS Instrument and is intended to measure apparent resistivity and/or induced polarization in direct current. Depending on the models, it allows 1D measurements (in manual mode), or 2D apparent resistivity panels (in automatic mode). The Syscal Pro 48 has both options and can carry out automatic measurements from a measurement protocol using a maximum of 48 electrodes.

For our study, we used it only in 2D mode to produce apparent resistivity panels.

- Data processing tools

These are essentially computer tools, intended for the configuration of measuring devices (Electre Pro), data collection and preprocessing (Prosys 2, X2IPI) and finally, the inversion in the specific case of tomography data.

The inversion software used for this study is DC2DInvRes (2.12.0, 2007), which is a free software developed by Thomas Gunther, and which operates in full options mode under a free license request from the developer (Gunther@resistivity.net).

2.2. Methods

The methodology applied at our study site is mainly focused on the implementation of geophysical investigations. However, due to the absence of data on the location of the dam, we wanted to first produce a map of lineaments which could potentially help understand the geophysical data.

2.2.1. Mapping of Site Lineaments

The detection of the lineaments of the site was realized under ENVI, by importing the ALOS PALSAR image corresponding to our site. The processing used to point out lineaments consisted of creating a colored composition and applying directional filters.

Due to the small size of our site, the lineaments were drawn manually and the detected anomalies were imported into SURFER for a combined display with the geophysical data.

2.2.2. Geophysical Prospecting

- Choice of measurement parameters

The main parameter used for the study of our site is resistivity expressed in Ohm.m. It is a parameter used in geophysics for the characterization of the electrical properties of subsurface materials [13]-[15]. It is made possible by the fact that the electrical properties of the soil layers are generally related to their porosity, their degree of saturation and/or the conductivity of the imbibition water [16].

For our site, the aim of geophysical prospecting was to understand the exchange processes between the lake and the embankment. We therefore used resistivity as a marker of the humidification process of the embankment and the downstream zone, with the objective of detecting any problems with the watertightness of the embankment.

With the equipment at our disposal, two types of apparent resistivity could be measured: DC electrical resistivity, obtained using Syscal Pro resistivimeter, and frequency-domain electromagnetic resistivity, measured using Max-Min II.

In association with electromagnetic resistivity measurements, the values of the in-phase and out-of-phase components of the secondary electromagnetic field were also recorded. They are actually used to detect vertical anomalies or contact zones between structures with contrasting electromagnetic properties [17].

- Exploration method

➢ *Electromagnetic prospecting*

Propecting with electromagnetic method was realized using Max-Min II. It consisted of trailing lines along the dam's embankment, with the following measurement configuration:

- Horizontal coil position, for maximum penetration of the primary field in the ground;

- Distance between transmitter and receiver: 100 m, to obtain the signal of a large volume of the subsoil, including bedrock response;

- Frequency used: 3520 Hz, for sufficient penetration depth to reach the bed-

rock;

- Measurement step: 20 m, for optimum sampling of lateral variations;

A total of three measurement profiles were realized, two downstream of the dam and one inside the dam basin. At each measurement point, three parameters were read: the in-phase and out-of-phase components of the secondary electromagnetic field, and the apparent resistivity of the subsoil.

➢ *Electrical Resistivity Tomography* (ERT)

The ERT measurements covered a transect located downstream of the embankment and offset by 5 meters from it. Using Syscal Pro, we realized apparent resistivity panels with Schlumberger protocol based on 48 electrodes.

Two types of exploration were realized:

- A terrain reconnaissance measurement covering 475 meters along the embankment. The distance was covered by a complete panel of 48 electrodes spaced 5 meters apart, extended by two Roll-Along acquisitions of 24 electrodes;

- A time-lapse monitoring which focused on a portion of the embankment located in the southern part and suspected to be a fragile zone. It consisted of two series of measurements (in a single panel), taken at different periods: one in the dry season (when dam was dry) and one in the rainy season (with the dam filled).

- Data processing and presentation of results

➢ *Electromagnetic prospecting data*

They were subjected to two types of processing:

- Manual input into an Excel spreadsheet, from which graphs were generated for each series of measurements taken along the profiles;

- Spatialization is done by kriging and display of electromagnetic field and resistivity data using Surfer software. Each parameter was displayed as a map.

➢ *ERT data*

The ERT data processing mode focuses on inversion calculations under DC2DInvRes using Gauss-Newton algorithm. Two types of calculations were performed:

A single inversion for the recognition panel data. The result of this inversion is presented in the form of a cross-section of calculated resistivities representing the 2D organization of the subsoil. This panel was interpreted to obtain a geological cross-section of the soil.

- A time-lapse inversion for temporal resistivity monitoring data, consisting of a succession of two single inversions (May and October data). Results for this inversion are presented in the form of resistivity ratios cross-section, between the two monitoring periods. Interpretation of the results is based on changes in the soil imbibition water properties, which can generate conductivity or saturation effects [18] [19].

3. Results and Discussions

3.1. The State of Fracturing of the Granite Basement in the Site

The study of subsoil fracturing on the site allowed the tracing of a certain number

of lineaments presented in Figure 3(A). They are preferably oriented, N15 and N45.

Among the lineaments identified on the site (nine), only two of them cross the dam installation area. On the map in Figure 3(A), it can be observed that they intersect in the center of the spillway. On the site, however, we did not observe any particular indications of the presence of a geological accident that could correspond to the identified lineaments. Observations are also made difficult by the fact that the site was greatly disturbed by the construction works of the dam: building of the embankment, spillway and ancillary works such as the development of the lake basin.

Therefore, the only way we had to associate these lineaments with possible geological anomalies was geophysical reconnaissance of the site.

3.2. Results of Geophysical Exploration of the Site

3.2.1. Electromagnetic Prospecting

The results of the electromagnetism exploration are presented here in individual profiles, and in maps.

For the presentation of the results by profile, all the measured parameters are displayed in a graph presenting the evolution of the measured values along the profile. The map presentation, on the other hand, is made by a type of parameter: resistivity and components of the secondary magnetic field in in-phase and out-of-phase.

- Measurements by profile

Graphs 3B, 3C and 3D (Figure 3) show the values measured along the three profiles positioned in parallel with the embankment of the dam. The location of the profiles, and the lineaments crossed by each of them, can be seen on the attached map 3A (Figure 3). For each measurement point, parameters recorded are: Secondary magnetic field components in in-phase and out-of-phase (%) and electromagnetic resistivity (Ohm.m).

➢ *Profile* 1

It is located downstream of the embankment (Figure 3(D)). Measurements taken along this profile show resistivity values of around 40 Ohm.m, with a major resistance anomaly (70 Ohm.m) near 180 meters' distance. On the graph showing the measured values, the points of intersection with lineaments 1 and 2 are indicated. It can be seen that they correspond to the limits of the major resistance anomaly. On the other hand, these boundaries do not seem to correspond to a clearly marked contact zone with neighbouring terrains. Indeed, measurements of the secondary field components (in-phase and out-of-phase) on this profile show slow, synchronized variations throughout. These measurements therefore, do not support the existence of a marked lithological contrast on this profile.

➢ *Profile* 2

This is the reconnaissance profile for the embankment installation area (Figure 3(C)). In this part of the site, the resistivity values read along the two sections of the embankment vary very little, and are close to 50 Ohm.m. These values contrast with those observed at the spillway, where a series of high values can be observed. Concerning secondary magnetic field components values, the shape of the curves at the spillway confirms the presence of an anomaly, but probably not a vertical

one (there is no clear inversion of the in-phase and out-of-phase curves). We therefore believe that, the subsurface geophysical response recorded in this area comes mainly from construction materials of the spillway, in particular the rockfill and the concrete areas located downstream of it.

➢ *Profile* 3

The results on this third profile (Cf; **Figure 3(B)**) were intended to compensate for the lack of geophysical response of the lineaments in the spillway area. However, the recorded data is more difficult to interpret on the profile scale. Indeed, the major resistant anomaly that appears through the resistivity curve does not correspond to any structure visible on the site. One of the explanations we came up with, was the response of the granitic basement, which would be closer to the surface at this point. The position of the two lineaments, as presented in the figure, is neither revealed by geophysical data nor by on-site observations.

Thus, when interpreting the data from the three profiles taken individually, it is difficult to draw a conclusion on the effective presence of geological accidents that could correspond to the two identified lineaments that cross the dam. Therefore, following these first analyses, we propose a spatial reading of the measured values.

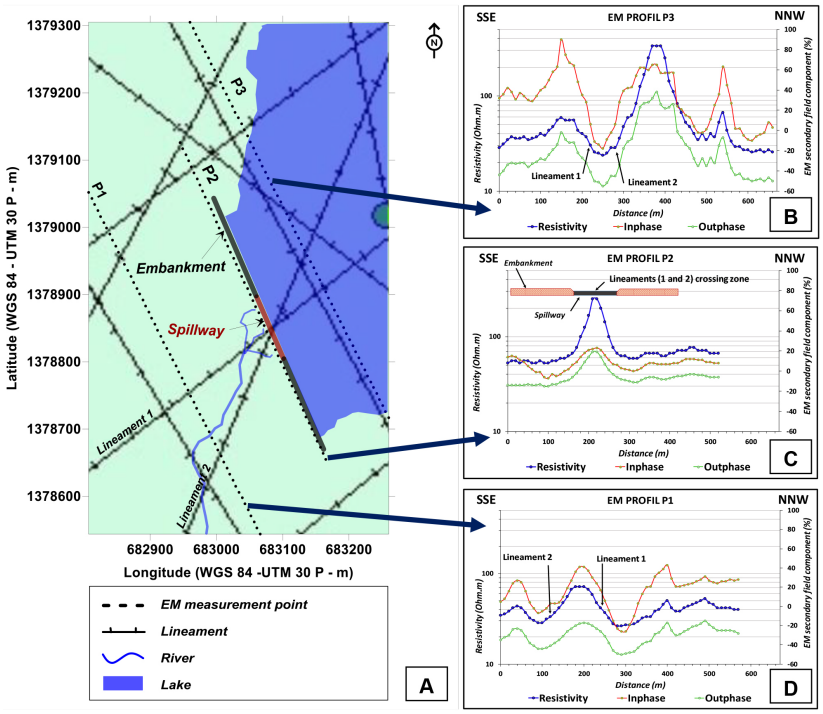

Figure 3. Map of site lineaments and electromagnetism prospecting results by profile. (Source: Alos Palsar images (2016))

- Spatialized data

The results of the spatialization of data from the three profiles are illustrated in **Figures 4 and 5**, which present three maps, each illustrating the organization of one of the three parameters measured.

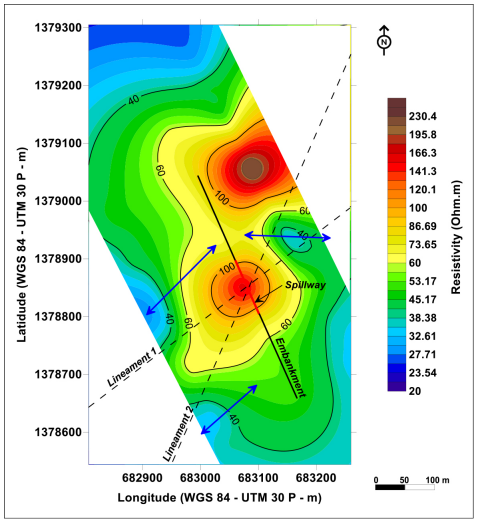

Figure 4. Apparent resistivity map of the site.

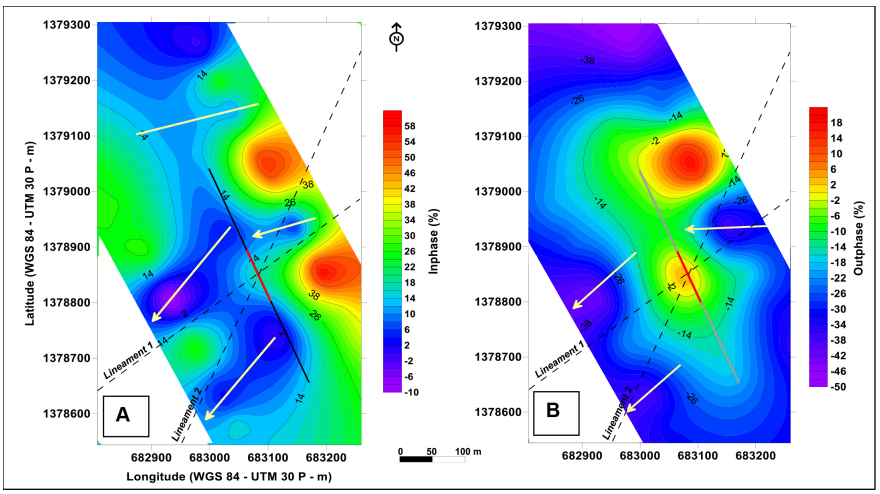

Figure 5. Maps of secondary electromagnetic field components. (A) In-phase; (B) Out-of-phase.

➢ *Resistivity map*

It is represented by **Figure 4**. On this map, we observe:

- A large resistant anomaly in the center of the prospected area, with a limit marked by the contour of the resistivity at 60 Ohm.m. Inside this anomaly, there are two small zones of high resistivity (100 Ohm.m), one located at the level of the spillway and the other inside the dam basin;

- Conductive zones are distributed around the central resistant anomaly. In the center and south of the site, they present growths that seem to converge towards the embankment route. This tendency towards linearity is materialized in the figure, by the arrows (in blue) which show the axis of extension of these conductive zones.

From this map, we notice that the embankment (and the spillway) is built on a generally resistant area, probably in a place where the bedrock is shallower. The

expected response of the two lineaments that cross the dam is not visible. On the other hand, new conductive anomalies appear, and their existence must be confirmed using the other parameters measured.

➢ *Secondary magnetic field components map*

The spatialized data of the components of the secondary magnetic field are represented in **Figure 5**: **Figure 5(A)** for inphase component and **Figure 5(B)** for outphase one.

On these two maps, we notice that the organization of the anomalies confirms the observations made on the conductivity map.

The phase map is more interesting because it better presents the variations of the secondary field, linked to the strong drops in resistivity. Indeed, through the negative variations of this component of the field, we can distinguish four anomalies, three of them corresponding to those already observed on the resistivity map. The fourth anomaly to the north of the site passes beyond the dam embankment and will not be taken into account in this study. Another striking aspect of this map is the role of the embankment. It seems to constitute the barrier from which the conductive anomalies start, particularly both downstream of the embankment (Cf; **Figure 5(A)**).

At the end of the exploration phase of the site, the first conclusions we draw are as follows:

- The study of the fracturing of the site shows that the dam site is crossed by two lineaments that intersect at the level of the spillway. However, field observations do not allow us to attest to their presence;

- Electromagnetic exploration of the site did not reveal any geological accidents that might be associated with the previously identified lineaments. However, this does not mean that there is no anomaly present on the site. This non-detection may be linked to the unsuitability of the method used or the way it was implemented (configuration of the measuring device, meshing of the site by the measurements) on the site, or to the nature of the lineaments, which may correspond to realities that have no geophysical signal (surface contrast, for example);

- The spatial analysis of exploration data, reveals conductive anomalies which originate from the embankment. The embankment is an artificial object in the landscape, and these conductive anomalies associated with it can therefore be considered as resulting from its installation. The basic explanation for this observation is the existence of water leakage through the embankment. The fact that the anomalies extend over several tens of meters, implies that the water leaks are significant and, above all, date back several years.

To verify the processes in progress downstream of the embankment, we analyze in the following paragraphs, the results of the resistivity tomography.

3.2.2. ERT Results along the Embankment

Electrical resistivity tomography deployed along the dam embankment, provided apparent resistivity data which, once inverted with DC2DInvRes software, gave

the results shown in Figure 6. It is a 2D cross-section of calculated resistivities representing the subsurface organization model according to resistivity parameter, whose values are illustrated here by color ranges: warm for high values and cold for low ones. Note also that, the image has a desired scale distortion (1/5), which favors depth representation.

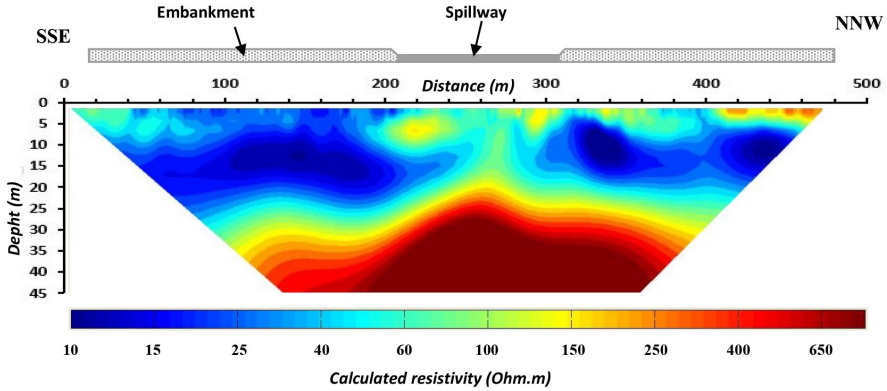

Figure 6. Calculated resisitivity cross-section along the embankment of the dam.

The displayed calculated resistivity section shows resistivity values ranging from 10 to 6500 Ohm.m, organized globally in tabular ranges. From surface to depth, we distinguish:

- A zone of high resistivity, with values ranging from 100 to 250 Ohm.m. This surface zone is discontinuous and shows variable thickness (3 to 10 m). It is most visible in the central part of the section, where it is also thickest (10 m). At the extremities of the section, it is thinner (3 m) and more resistant (250 Ohm.m).

- A thick conductive layer (10 to 60 Ohm.m) running south to north, from depths between 5 and 30 m. The interior of this layer is marked by the presence of two highly conductive zones (10 to 20 Ohm.m) that extend in the direction of the layer and are separated by a resistant zone in the center of the section. These highly conductive zones are often exposed in the southern part of the section, and less so in the northern part.

A highly resistant layer (over 400 Ohm.m) at depth over 35 meters, topped by a less resistant transition zone (150 to 400 Ohm.m).

By plotting the position of the embankment of the dam on the resistivity cross-section, we notice that the concrete spillway is located at the level of the resistant zone (100 to 150 Ohm.m) located in the middle of the resistivity cross-section. The two parts of the earth embankment, on the other hand, are located in zones of contrasting resistivities: In the southern part, most of the base of the embankment is in contact with a very conductive zone. The north portion, on the other hand, is in contact with a resistant zone with a conductive breach at around 400 meters.

In the absence of an observation borehole, which could not be drilled along the dike without special arrangements (authorization requests), we propose in Figure 7, an interpretation of the resistivity cross-section which results from obser-

vations made throughout the site (surface observations, profiles of artisanal wells and termite mound materials) but also from our knowledge of the study area in general.

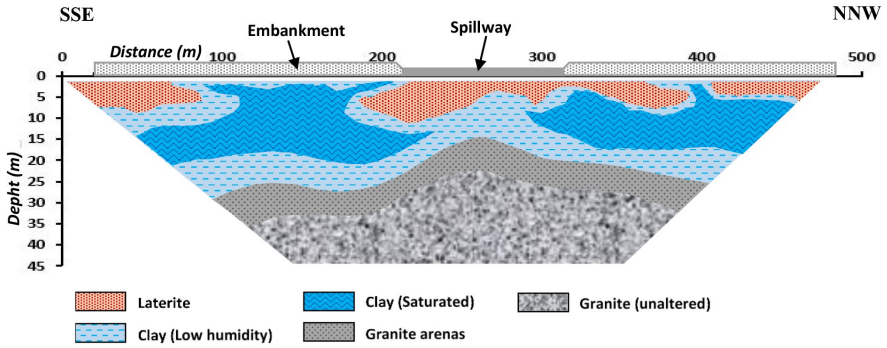

Figure 7. Interpretation of the calculated resistivity cross-section.

In the proposed interpretation, four types of terrain are distinguished. However, their boundaries may not correspond to changes in nature, but rather to changes influenced by the water content and/or electrical conductivity of the imbibing water, as it is known, resistivity largely depends on these factors.

- At the surface, the resistant layers correspond to outcropping lateritic horizons, which are in some places, covered by thin silty-clay layers (20 to 50 cm). Their thicknesses as observed in the wells or the over-digging of the watercourse downstream of the dam, are around a meter, while the resistivity cross-section shows greater thicknesses (up to 5 m or more, at the level of the spillway). This suggests that the lateritic layer, in the vicinity of the dike, is not natural but probably created or reinforced by addition of materials used for the installation of the embankment. This also explains the particularly thick layer of the lateritic layer at the level of the spillway. At this location on the site, it can be seen that, in addition to the laterite, rubble and boulders were added to stabilize the dissipation basin downstream of the spillway. Finally, field observations show that the lateritic layer is continuous. Therefore, the discontinuities that appear on the resistivity section seem to result from differences in the state (especially water content) of the layer.

- Based on the displayed resistivity values and field observations, particularly materials extracted from artisanal wells and those constituting termite mounds, we concluded that the layer below the lateritic one is clayey. It is an ocher to whitish clay (as observed in artisanal wells) reaching 20 to 25 m thick, within which, the very low resistivities (marked in darker blue) would result from a higher water content. This can be verified at some points such as the southern part of the embankment, where wetter parts of the layer reach the surface. These areas correspond to marshy places in the rainy season;

- At the bottom of the cross-section, high resistivities are associated with the granitic bedrock characteristic of the study site. Above this bedrock, intermediate resistivities are associated with granitic arenas.

The whole of the proposed interpretation refers to the fairly classic profile model of a leached tropical ferruginous soil with an average weathering depth of 25 meters. However, some aspects of the proposed model do not correspond exactly to what is commonly observed on a natural soil profile.

Indeed, the thickness of the superficial lateritic layer appears here to be quite considerable, suggesting that it is not entirely natural. Because the geophysical measurements were taken just downstream of the embankment, we believe that the thickness of the surface lateritic layer is explained by the addition of laterite used as fill material for the construction of the embankment.

Furthermore, it seems illogical that this backfill has such varying thicknesses and be so fragmented along the embankment, as shown by the interpretation in Figure 7. Explanation which can be given here, is that the appearance of the backfill layer, as reflected by the resistivity, does not correspond to the actual structure of the soil. Indeed, knowing that resistivity is influenced by the water content of the materials, it is highly plausible that the conductive parts observed in the backfill, correspond to zones of high water content. The connection observed between the conductive zones on the surface and those at depth, would therefore be linked to a similar water content in these areas. This suggests that the backfill layer is quite continuous, as presented in Figure 8. Its thickness would be fairly uniform in both parts of the dike, and greater at the spillway, where we believe the backfill is reinforced.

In Figure 8, the superposition of zones with high water content and the lateritic layer provides a better illustration of the parts of the backfill affected by fairly pronounced wetting. Three zones stand out:

- The southern part of the embankment, from a distance of 90 meters to the contact zone with the spillway at 200 meters. At this point, moisture affects a large part of the base of the embankment;

- The area below the spillway. The measurements taken here do not show a rise in humidity up to the level of the concrete part of the spillway. However, field observations show the existence of the Renard phenomenon at the base of the spillway. Patching work even seems to have been carried out, but apparently, without much result (the scours are still clearly visible);

- The small area is within a 400-meter distance. It is a small subvertical rise which extends over a few meters at the base of the embankment.

Below the backfill layer, we can also observe that, the zone considered to have a high water content, constitutes a continuous layer that stretches along the interpreted section. It could be an aquifer seasonally recharged largely by water from the dam. Knowing that the tomography measurements were carried out in May, the level of this water table, as seen in the section, would correspond to its lowest level. It is therefore very likely that at the end of the rainy season (in October), the level of this water table rises sufficiently to invade the entire embankment, helped by the water level in the dam, which at this period is at its maximum.

For a better understanding of the action of the rise of the water table and the pressure of the water from the dam which weakens the dike over time, we present in the following paragraphs, the results of the time-lapse monitoring tests carried out on the south part of the embankment.

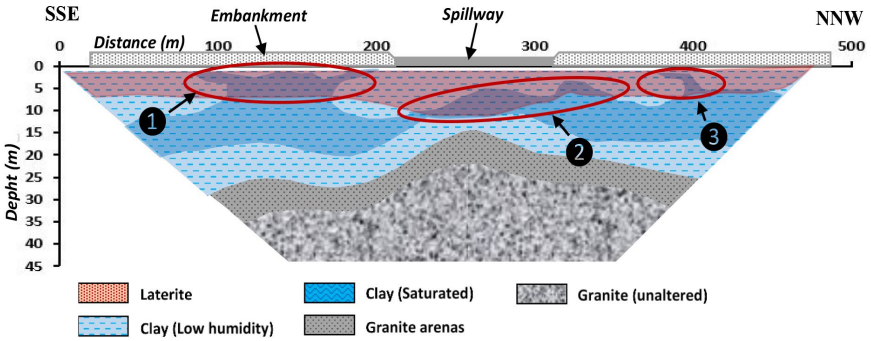

Figure 8. Reinterpretation of the resistivity cross-section by assuming the continuity of the surface layer and taking into account variations in water content in the layer.

3.2.3. Time-Lapse Monitoring Results

Time-lapse resistivity monitoring focused on the southeast portion of the embankment located between distances 0 and 235 meters (Cf; **Figure 9(A)**).

The measurements carried out in this part of the embankment, aimed to monitor possible resistivity variations, which would exist between the dry and the rainy season and could help to improve the understanding of the transfer processes between the lake and the embankment.

The results presented relate to measurements at the end of the dry season (May) and those at the end of the rainy season (October) for the year 2021.

- May results

Figure 9(B) presents the calculated resistivities for measurements realized in May. On the resistivity cross-section, the presence of the superficial conductive zones over almost the entire length of this portion of the embankment is clearly visible. We can also notice their connection with the large conductive zone deeper.

In the monitoring area, the soil surface at the time of measurements was apparently quite dry. However, the portion between 70 and 100 meters was wet, even muddy in some places.

- October results

Measurements in October (25th of the month) were carried out in very wet soil conditions. Apart from the first 20 meters of the profile, the rest was muddy.

The calculated resistivity cross-section (**Figure 9(C)**) shows a generalized increase of resistivities over the first 5 meters, which is clearly visible at the beginning and end of the section. The large conductive zone in the center of the image, also shows a reduction in its size.

For the deep parts of the section however, it does not seem to have any visible dynamics.

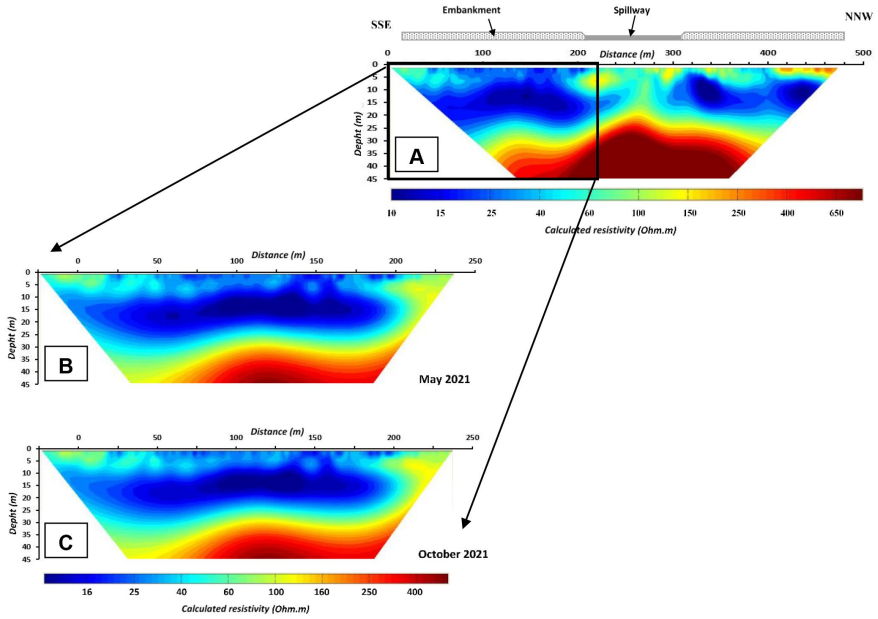

Figure 9. Time-lapse monitoring results for May and October. (A) Monitored part of the embankment; (B) Calculated resistivity section for May; C) Calculated resistivity section for October.

- Ratio of resistivities (October/May)

Figure 10 presents the ratio of resistivities for October compared to those of May. Variations are given in percentages and presented according to a color scale ranging from cold tones (for decreases), to warm tones (for increases).

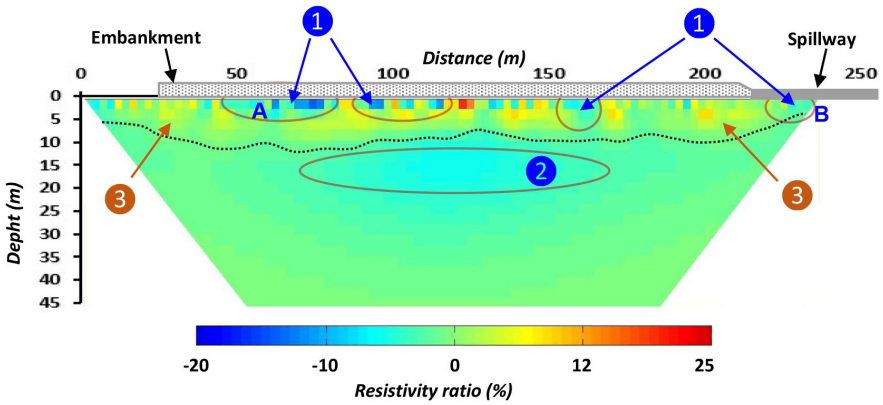

Figure 10. Resistivity ratio cross-section (October/May).

From the section of the resistivity ratio, the following observations can be made:

- Resistivity variations between the end of the dry season (May) and the end of the rainy season, range from −20 to 25%;

- Most of the variations occur at depths between 0 and 10 meters (zone 3 on Figure 10). Resistivity rises are particularly noticeable along the entire length of the section. The lower limit of this zone (delimited by the dotted line) is quite irregular;

- At the surface, we observe along the section, four zones of decreasing resistivities (zones 1) which contrast with the dominant resistant zones. It concerns the area between 50 and 75 meters, around 100 and 160 meters and finally, that below the spillway.

- Beyond the depth of 10 meters and in the center of the section, another zone of decreasing resistivity is also observable (zone 2). The decrease in this zone, is however, low (around 5%).

- In the deeper areas of the section, variations are minimal or non-existent.

In order to understand the dynamics of resistivity variations in this section of the embankment, we'd like to provide some background information on the operation of the dam.

This resistivity effect can be observed at the surface of the time-lapse ratio cross-section (zone 3). It results in an increase of resistivity caused by the quality of the infiltrated water which is resistant: water, taken from an artisanal well near the site, had a resistivity of 170 Ohm.m in October. Assuming that the embankment is watertight, impregnation water in the layers downstream the embankment would therefore, be from the recently-completed rainy season. The reason why the effect of water resistivity is so visible at this level of the ground would come from the fact that, surface layers are transit zones and therefore are not saturated (less saturation effect).

Assuming that the increases of resistivity in the upper layers are induced by resistivity effect of rainwater, the existence of superficial zones of resistivity decreases (zone 1), raises questions about these differences. The explanation we found is based on the difference in soil water content. We think that, what is observed at this location corresponds to the saturation effect. This is possible in places where soil moisture levels remain particularly high throughout the year (also the case in zone 2, deeper). Knowing that there is no zone of water stagnation along the embankment, we can therefore conclude that these zones of reduced resistivity, simply correspond to places constantly moistened by water leaks through the embankment. For the area between 50 and 75 meters on the monitoring cross-section, the leak is actually visible on the site.

For the monitored part of the embankment, there are four zones of fragility (zone 1) as shown in **Figure 10**, and two of them are actually visible on site: zone 1A at embankment level, and zone 1B below the spillway.

The leak on the embankment side is clearly visible because it creates a wetland (downstream of the dike) with grasses that are sometimes still green at the end of the dry season (Cf; **Figure 11(A)**).

At the spillway, the monitoring results show that the leakage does not occur in the contact zone between the embankment and the spillway (dam failures often occur at these points), but rather under the spillway. Consequently, the leakage observed at this level does not immediately threaten the safety of the embankment. On the other hand, the damage to the spillway is already considerable, with the concrete zone collapsing, downstream (Cf; **Figure 11(B)**).

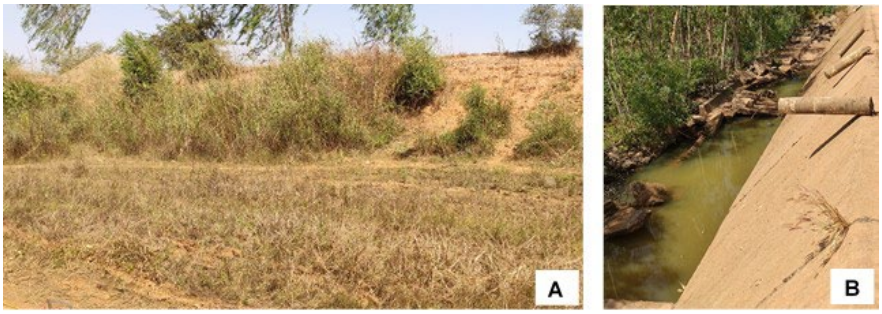

Figure 11. View of areas affected by water leakage. (A) Downstream of the southern section of the embankment. This area remains wet all year round, benefiting the grass and shrubs that persist on the soil and embankment throughout the year. (B) Downstream of the spillway. The persistence of water at this location during the dry season (February) indicates the presence of water leaks below the spillway. The damage we also observe there, is doubtless partly caused by these leaks.

Based on the monitoring results for the southern section of the embankment, it can be said that time-lapse resistivity monitoring has enabled us to obtain details of the weak areas of the embankment that appeared on the electromagnetic prospecting maps.

It is now known that, this part of the embankment has enough fragile zones that deserve to be taken into account for rehabilitation work or a check of the condition of the structure.

With these results, we can also predict the state of ageing of the remaining section (northern part) of the dike, which was not subject to resistivity monitoring. With already a known point of fragility in this section (zone around 400 meters on the profile), it is very likely that additional measurements, will bring more details and/or reveal additional pathologies.

4. Conclusions

The diagnostic study of the Gonsé dam revealed the state of the structure, which visually showed signs of advanced degradation in some of its compartments.

The mapping of the lineaments we carried out, showed that the site contained probable geological accidents passing through the concrete spillway. However, geophysical measurements have not confirmed their presence or even given any indication of their impact on the structure. Despite this observation, we believe it is important to take these lineaments into account in the event of the need for further diagnostics or rehabilitation work on the dam, given that the geophysical exploration method we used also has its limitations.

By deploying the electromagnetic method on this site, we succeeded in highlighting the areas of fragility of the dam embankment. When processing the data from this survey, we realised that it was preferable to interpret the data spatially rather than by a measurements profile. Among the electromagnetic parameters measured, the in-phase component is the one that best presents the desired anomalies. This is, therefore, a factor to be taken into account for a preliminary analysis

of the results.

Our results have also shown that, with electrical resistivity tomography, we obtain a better overview of the anomalies through cross-section presentation. Then, carrying out temporal monitoring of resistivity at the level of these anomalies, allows us to confirm their presence and obtain more details on their extension.

We can therefore validate the exploratory method used for this site, as being suitable for routine preliminary diagnosis of small dams. It is non-invasive, uses a lightweight device and is quick and easy to implement. We recommend that electromagnetic measurements be carried out on a few profiles for preliminary detection of anomalies, followed by resistivity tomography to pinpoint areas of water leakage through the embankments. If time is available, this routine can be supplemented with temporal resistivity monitoring.

By studying this small dam, we also hope that the results will be a first step towards a better understanding of how the country's many small earth dams operate and age. This would enable us to anticipate certain problems associated with the deterioration of the structures and to be better prepared for routine maintenance or rehabilitation work.

Conflicts of Interest

The authors declare no conflicts of interest regarding the publication of this paper.

References

[1] Mei, L. (2003) La ressource en eau au Burkina Faso gestion et enjeux. *Travaux du Laboratoire de Géographie Physique Appliquée*, **22**, 37-55. https://doi.org/10.3406/tlgpa.2003.1010

[2] Cecchi, P. (2006) Les petits barrages au Burkina Faso: Un vecteur du changement social et de mutation des réalités Rurales. Pré forum mondial de l'eau. Institut de Recherches pour le Développement, 12 p.

[3] Ministère de l'Environnement, de l'Eau et de l'Assainissement-Burkina Faso (2011) Mise à jour des donnees sur les retenues d'eau de surface. MEAHA/DGRE/DEIE, Rapport Technique, 35 p.

[4] Ministère de l'Environnement, de l'Eau et de l'Assainissement-Burkina Faso (2022) Stratégie nationale d'entretien et de sécurité des barrages (SNESB) au Burkina Faso: Horizon 2023-2027. MEEA, 167 p. https://www.mea.gov.bf/fileadmin/user_upload/stockage/documents/Document_Cadre_Entretien_et_Securite_des_Barrages_au_BF_version_Finale.pdf

[5] Durand, J.M., Royet, P. and Mériaux, V. (2023) Technique des petits barrages en Afrique sahélienne et équatoriale. Cemagref Editions, 415. https://hal.inrae.fr/hal-02578000

[6] Beck, Y.L., Khan, A.A., Cunat, P., Guidoux, C., Artières, O., Mars, J. and Fry, J.J. (2014) Thermal Monitoring of Embankment Dams by Fiber Optics. 8*th ICOLD European Club Symposium*, Innsbruck, September 2010, 444-448.

[7] Benfetta, H., Achour, B., Boudina, S., Hocini, N. and Ouadja, A. (2017) Techniques de détection du cheminement des fuites dans les barrages et autres réservoirs artificiels. *Larhyss Journal*, **14**, 361-390. https://asjp.cerist.dz/en/article/55649

[8] Camarero, P.L. and Moreira, C.A. (2017) Geophysical Investigation of Earth Dam

Using the Electrical Tomography Resistivity Technique. *REM-International Engineering Journal*, **70**, 47-52. https://doi.org/10.1590/0370-44672016700099

[9] Dahlin, T., Sjödahl, P. and Johansson, S. (2008) Embankment Dam Seepage Evaluation from Resistivity Monitoring Data. *Near Surface* 2008-14*th EAGE European Meeting of Environmental and Engineering Geophysics*, Kraków, 15-17 September 2008, 463-474. https://doi.org/10.3997/2214-4609.20146268

[10] Savadogo, A.N., Descloitres, M., Nakolendousse, S., Camerlynck, C., Bazie, P., Le Troque, Y. and Koussoube, Y. (2001) Etude géophysique du tracé de la digue du futur barrage de Yakouta au Burkina Faso. Complémentarité des méthodes électriques et radar en milieu dunaire. 3*e Colloque GEOFCAN*, Orléans, 25-26 September 2001, 4 p.

[11] Nakolendousse, S., Yaméogo, S., Savadogo, A.N. and Koussoube, Y. (2009) Contribution des mesures géophysiques électriques et électromagnétiques dans l'étude du site du barrage de Samendéni: mise en évidence de failles et d'intrusion de dolérites. *Sécheresse*, **20**, 232-236. https://doi.org/10.1684/sec.2009.0188

[12] Noumpoa Karambiri, B.L.C. and Gansaonre, R.N. (2023) Variabilité Spatio-Temporelle de la Pluviométrie dans les Zones Climatiques du Burkina Faso: Cas de Bobo—dioulasso, Ouagadougou et Dori. *European Scientific Journal, ESJ*, **19**, 262. https://doi.org/10.19044/esj.2023.v19n9p262

[13] Goulet, E. and Barbeau, G. (2006) Apports des mesures de résistivité électrique du sol dans les études sur le fonctionnement hydrique du système sol/vigne. *Journal international des sciences de la vigne et du vin*, **40**, 57-69.

[14] Paillet, Y., Cassagne, N., Cecillon, L., Breton, V., Mermin, E., *et al*. (2008) La Résistivité Electrique: Une nouvelle méthode de cartographie de certaines propriétés des sols forestiers et des formes humus. *Rendezvous Techniques de l'ONF*, No. 4, 48-50. https://hal.science/hal-00478430v1

[15] Kouakou, A.K., Kouamé, N.L., Djroh, S.P., Kouadio, L.K. and Sombo, C.B. (2017) Utilisation de la méthode de resistivité électrique pour la recherche de carrières granitiques et estimation du tonnage rocheux sur trois sites: Ayame, Bouake et Ferkessedougou (Côte d'Ivoire). *International Journal of Technical Research and Applications*, **5**, 40-46.

[16] Archie, G.E. (1942) The Electrical Resistivity Log as an Aid in Determining Some Reservoir Characteristics. *Transactions of the AIME*, **146**, 54-62. https://doi.org/10.2118/942054-g

[17] Jolivet, A., Nguyen, V.H. and Tabbagh, A. (1977) Utilisation de la phase dans la méthode de prospection électromagnétique S.G.D. *Revue d'Archéométrie*, **1**, 115-126. https://doi.org/10.3406/arsci.1977.1085

[18] Clément, R., Descloitres, M., Günther, T., Ribolzi, O. and Legchenko, A. (2009) Influence of Shallow Infiltration on Time-Lapse ERT: Experience of Advanced Interpretation. *Comptes Rendus. Géoscience*, **341**, 886-898. https://doi.org/10.1016/j.crte.2009.07.005

[19] Wubda, M., Descloitres, M., Yalo, N., Ribolzi, O., Vouillamoz, J.M., Boukari, M., *et al*. (2017) Time-Lapse Electrical Surveys to Locate Infiltration Zones in Weathered Hard Rock Tropical Areas. *Journal of Applied Geophysics*, **142**, 23-37. https://doi.org/10.1016/j.jappgeo.2017.01.027